

ROLE OF COMPUTATIONAL FLUID DYNAMICS IN THE DESIGN OF AEROSPACE CONFIGURATIONS

S. K. Chakrabartty*

Abstract

Computational Fluid Dynamics (CFD), a mature discipline now, can contribute considerably to the design, analysis and development of engineering systems involving fluid flows. Visualization of flow-field, surface load distribution and various aerodynamic forces and moments are the criteria for basic design of aerospace configurations. CFD complements experimental and theoretical fluid dynamics by providing an alternative and cost effective means to simulate real flow phenomena. The main advantage lies in its ability to cut down the number of wind-tunnel tests leading to reduction in the design cycle time and design cost. After a brief introduction to CFD, the role played by the modern CFD tools developed at the Computational and Theoretical Fluid Dynamics Division of National Aerospace Laboratories, Bangalore in the design and analysis of Aerospace configurations will be discussed here.

Introduction

The subject Computational Fluid Dynamics (CFD) is a hybrid technology based on the knowledge and experience on fluid dynamics, numerical analysis, fundamentals of partial differential equations, thermodynamics and computer science. CFD of aerospace interest deals with numerical solution of the equations governing compressible fluid dynamics. Pioneering works of Magnus and Yoshihara [1] and Murman and Cole [2] laid the foundation for solving transonic small perturbation equation which is non-linear and mixed-type partial differential equation. The distinguishing feature of transonic flow field is that both subsonic and supersonic regions are present in the flow adjacent to each other and that these fields are significant in determining the overall character of the flow field. Type dependent differencing introduced in [2] was the key to success in computing transonic flows. On the other hand, Pearcy [3], Nieuwland and Spee [4] and Spee and Uijlenhoet [5] succeeded in obtaining shock-free transonic flow past aerofoils. Later, the famous supercritical Korn aerofoils [6] were successfully designed using hodograph method for transonic full potential equation. This method has the limitation that it cannot be extended either to viscous flow or to three-dimensional flow. The off-design behaviour of the supercritical Korn aerofoil in viscous transonic flow has been studied by Chakrabartty and Dhanalakshmi [7]. For aerofoil design, this type of flow is of great interest in view of the possibility of economic benefits at higher cruising speeds without suffering the drag penalty when a significant amount of

supersonic region is present together with a stationary weak shock or no shock at all. From physical point of view, it is interesting to know if a given shock-free transonic flow past a profile possesses shock-free solution for neighboring values of the free stream Mach number (well known transonic controversy, [8]). However, in order to develop efficient designs, it is necessary to understand the aerodynamic behaviour that occurs at transonic speed range. Accurate analysis and understanding of the flow field play a significant role in efficient design process. A simple hodograph method for the design of shock-free supercritical aerofoils using Rheoelectrical Analogy and Characteristic Methods (RACM) was developed at NAL [9] and a few super-critical aerofoils were successfully designed. Design of Natural Laminar Flow (NLF) aerofoils suitable for light transport aircraft was also initiated at NAL [10,11] and a series of NLF aerofoils was designed. These simple methods having capabilities to design aerofoil shapes for a given pressure distribution are no more in practice due to the appearance of advanced CFD tools in the field. Direct design / inverse methods where an aerofoil shape is sought for a given flow field at some free-stream condition are not so popular because the existence and uniqueness of the solution is not guaranteed. Recent interest in aerodynamic shape optimization is growing fast due to the fact that CFD is making fast progress using advanced computer technology and available efficient numerical algorithms [12]. In India, computational activities of transonic flow past aerofoils was initiated by Niyogi and Mitra [13] and Chakrabartty

* Computational and Theoretical Fluid Dynamics Division, National Aerospace Laboratories, Post Box No. 1779 Bangalore-560 017, India, Email: drskc@ctfd.cmmacs.ernet.in

[14,15] using integral equations method [16]. Later, scientists at National Aerospace Laboratories, Bangalore became interested in transonic flow both for analysis and design of aerofoils [17]. Since then, a process of continuous evolution of the activities was continued starting from two dimensional transonic small perturbation equation, transonic full potential equation, Euler equations and finally culminating in Reynolds Averaged Navier-Stokes (RANS) equations in both two and three dimensional flow past configurations of aerospace interest.

Under the assumption of continuous media, Reynolds Averaged Navier-Stokes (RANS) equations with a suitable turbulence model can be accepted as valid equations governing the fluid flows in general. There are sources of inaccuracies, such as getting suitable grid for complex geometries, uncertainty of the turbulence models used, etc. Even with an impressive progress in CFD, there continues to be, in aerodynamic design effort, a very useful, practical and even unavoidable slot for some of the classical approximations in aerodynamics and fluid mechanics, for low-order CFD codes, empirical data and also, importantly, for some amount of wind-tunnel testing. A holistic approach is essential and it requires certain effort to avoid the temptation of seeking a possible numerical solution from the latest CFD codes solving RANS equations at every stage of design. As Desai [18] has rightly pointed out, RANS cannot be the answer to all situations. It is not wise to solve RANS equations in every intermediate, interactive stage of an aircraft design. For complex flows, accuracy cannot be guaranteed simply because RANS equations have been solved. The basic features of the fluid flows of aerodynamic interest can be simulated by the Euler equations, obtained from the RANS equations by ignoring viscous effects. Euler equations can handle the rotational flows but there is no mechanism to generate vorticity. Some extreme views have been expressed in the literature such as wind tunnel testing may play a secondary role in the development of aircraft. But in reality, both CFD and wind tunnels are inevitable; there are roles which are exclusive for CFD and wind tunnels and there are roles which are synergistic and complementary to each other. It can be argued that the efficacy of CFD in aircraft design is to be judged not so much by the number of wind tunnel blow downs that can be saved but by the value addition to the design cycle by its contribution to a superior baseline for final tuning and check-out of configuration through detailed wind tunnel testing and by guidance obtainable through rapid CFD simulation for better utilization of tunnel tests [19].

A complete CFD process consists of i) Pre-processing and grid generation, ii) Numerical solution of the governing equations and iii) Post-processing of the solution. It is convenient to use the available commercial codes for grid generation and for post processing of the results. Grid generation software like GRIDGEN can be used to generate a multi-block structured or unstructured grid around a complex three-dimensional geometry. For post processing TECPLOT and CFDVIEW codes are suitable tools which enable the users / designers to visualize complex flow structures or to get aerodynamic coefficients with load distribution on a particular surface. These three codes are popular in the CFD community of NAL because of their multiple options and user-friendliness. In spite of having these sophisticated tools one has to develop many small codes during pre- and post-processing stage to convert data to a form acceptable by these codes. Indigenous codes are preferable for solving the governing equations in fluid dynamics at different approximation levels. Governing equations to be solved should be chosen from the various approximation levels of the RANS equations so as to satisfy the requirements of the designer.

Indigenous CFD Codes

Structured multi-block grid generation code JUMGRID can generate a multi-block grid for any arbitrary, geometrically complex body, for both external and internal flows. The grid is structured in any particular block but the blocks may be unstructured. The geometry data for a complex configuration is generally available for each component separately, sometimes in its own coordinate system. The code JUMGRID adopts the following steps to achieve the desired multi-block grid.

1. Read geometrical data for each component.
2. Redefine complete geometry in global coordinate system.
3. Form blocks suitable to the geometry and the topology intended.
4. Define all six faces in each block.
5. Redistribute points on each face as necessary.
6. Fill up initial internal points in each block.
7. Establish inter-block connectivity / boundary condition.
8. Smooth the grid by solving elliptic equations.

The code has been validated extensively by generating grid for SARAS wing-fuselage configuration, for an axi-

symmetric probe used in LCA and delta-wing with deflected aileron [20].

The solver codes JUEL2D and JUEL3D solve two and three dimensional Euler equations, whereas JUMBO2D and JUMBO3D solve two and three dimensional RANS equations respectively. A novel cell vertex finite volume method is employed for the solution of the equations. A five stage Runge-Kutta scheme has been used to advance the solution in time. Enthalpy damping, implicit residual smoothing, local time stepping, and grid sequencing are used for convergence acceleration. For turbulent flows, algebraic eddy viscosity model with proper correction for separated flows has been used. The computations can be carried out block-wise after dividing the computational domain into smaller blocks to reduce the memory requirement for a single processor computer and also to facilitate parallel computing. The codes are written in FORTRAN and can be run on any platform that supports standard FORTRAN.

These codes have been applied to a variety of problems during the last ten years [21,22,23,24]. The following are some of the examples solved by these codes:

1. Analysis of transonic flow past aerofoils including study of shock induced separation at the foot of a strong shock,
2. Analysis and design of aerofoil with flap configurations (GA(W)-2 and HANSA-3),
3. Internal flows through nozzles and cascades,
4. Euler analysis of ASLV-GSLV launch vehicles, Mig-21(Bis) wing-fuselage and nose radome of Jaguar aircraft,
5. Navier-Stokes analysis of round leading edge delta wing at high angles of attack and
6. Design and analysis of complete SARAS aircraft with side-slip. The presentation will demonstrate the use of Computational Fluid Dynamics as a scientific research tool for better understanding of the complex fluid flow phenomena and also as a design and analysis tool to serve the aerospace industry.

Results and Discussions

Supercritical and NLF Aerofoils

Shock-free supercritical aerofoils were reckoned as advanced technology concept in seventies. These aerofoils, designed theoretically, show shock-free flow at high

subsonic free stream condition called design condition. A conventional aerofoil, leads to flow separation and sudden rise in drag as the free stream Mach number exceeds the critical value and the supersonic region in the flow terminates with a shock. Many supercritical aerofoils designed so far are available in the literature [3-6, 9]. A shock-free lifting aerofoil at design conditions, $M_\infty = 0.806$, thickness to chord ratio $t/c = 0.075$, $C_1 \approx 0.39$ and $\alpha = 0^\circ$ using the RACM design procedure developed at NAL is shown in Fig.1 along with the analysis results at off design conditions. Another class of aerofoils called natural laminar flow (NLF) aerofoils were designed using an inverse design procedure suitable for NAL's civil aircraft projects. The pressure distribution obtained for MSNLF-150 aerofoil is shown in Fig.2. It is to be noted that this aerofoil has laminar flow beyond 50% of chord on both upper and lower surfaces. The super critical aerofoils designed for transonic flow are very sensitive to small changes in either the angle of attack, α , or the free-stream Mach number, M_∞ . Experimental results show the existence of double shocks at off-design conditions and it is still a difficult task to capture these double shocks through viscous flow computation [7]. Fig.3 shows the distribution of pressure coefficient C_p on a supercritical Korn aerofoil for $M_\infty=0.75$, $Re_\infty=5.42 \times 10^6$ at angles of attack ranging from -0.2° to 0.9° . The first shock appearing near the leading edge moves downstream whereas the second shock remains stationary but its strength decreases with increasing α . At $\alpha = -0.3^\circ$ and -0.4° a shock-like behaviour was observed near the leading edge but the second shock vanishes giving a smooth transition from supersonic to subsonic flow.

Vortex Flow Over Cropped Delta Wing

The capability to capture and analyze the complex flow accurately using CFD is necessary in the overall design process. To demonstrate the capability of NAL codes to predict complex flow structure accurately a typical example of complex flow past a round leading edge delta wing at high angle of attack has been considered [23]. The complete physics of the vortex breakdown and asymmetric vortex formation, over a symmetric, slender body at high angle of attack, is still a subject of research for both experimental and numerical studies. The main feature of the flow is the leeward vortices, formed by the rolling up of the shear layer in a spiral fashion, which occur in counter rotating pairs as the flow is shed about opposite leading edges. The primary separation originates close to the apex and inboard of the leeward side of the wing, and gradually moves closer to the leading edge further down-

stream. Due to the low pressure induced by these vortices on the wing surface, the flow experiences an adverse pressure gradient in the cross-flow direction towards the leading edge. This causes the secondary separation depending on the condition of the boundary layer, and also formation of a cross-flow shock depending on the free-stream conditions. Due to the property of turbulent flow to delay boundary layer separation, the secondary vortex in a laminar flow lies inboard of its position in a turbulent flow. Interaction with the cross-flow shock causes the boundary layer separation to reduce to a small separated bubble sitting at the foot of the shock, which reattaches inboard of the leading edge. Depending on the position of reattachment, a tertiary vortex may appear in the same orientation as the primary vortex. Further downstream of the flow, when the secondary vortex meets the terminating shock, it reduces further and gradually gets dissipated. Skin-friction lines on the upper surface of the wing for $M_\infty=0.85$, $\alpha=10^\circ$ and $Re_\infty=2.38 \times 10^6$ is shown in Fig.4. Primary and secondary separation and reattachment lines along with the formation of nodal and saddle points have been predicted by the RANS solver code JUMBO3D and shown in the figure. For the same case, surface pressure contour along with the streamlines originating near the leading edge are shown in Fig.5. Primary and secondary roll up vortices with opposite orientation are clearly visible. Particle traces on the cross-flow planes are shown in Fig.6 with the surface pressure contours on the surface. The primary vortex core at different cross-flow planes are shown.

Aerofoil-flap Design for HANSA-3

Effectiveness of the control surfaces is of critical importance for any aircraft. A design and analysis study of the flow past two-dimensional aerofoil with flap [21] is presented here. Since the basic aerofoil is the same in SARAS and HANSA-3 aircraft the present study is useful for both the aircraft. For the existing aerofoil flap configuration, a large separated region was predicted by the analysis code, JUMBO2D, which resulted in reduction of lift and loss of control effectiveness of the flap. This prompted us to look into the possibility of redesigning the configuration.

A comparison of existing and modified profiles of the main aerofoil and the flap is shown in Fig.7. Fig.8 shows the aerofoil with the flap deflected at $\delta = 0^\circ$, 10° , and 20° . Variation of computed lift coefficient C_L with α has been shown in Fig.9 for the same three positions of the flap for $M_\infty=0.3$, $Re_\infty=2.0 \times 10^6$. It is to be observed here that the

modified configuration shows almost a linear behaviour in the attached flow region and the maximum C_L increases with the increase in flap deflection. Comparison of the flow pattern between the existing and modified configurations with streamlines superimposed on pressure contours at $\alpha = 10^\circ$ for $\delta = 0^\circ$ and 20° are shown in Fig.10 and Fig.11 respectively. For $\delta = 0^\circ$, both the configurations show attached flow whereas for $\delta = 20^\circ$, the existing configuration exhibits a large portion of separated region over the flap and the modified configuration shows a very smooth behaviour having fully attached flow throughout with a small cove vortex in the gap close to the trailing edge of the main aerofoil. Comparisons of lift and drag coefficients of existing and modified aerofoil-flap configurations for different α are shown in Fig.12. It is to be observed that performance of the modified configuration with respect to the aerodynamic forces is much better in comparison to that of the existing one.

Wing-Fuselage-Fairing Modification for SARAS

In order to minimize the mutual interference effects of the wing and fuselage, it is very critical to design the wing-fuselage junction to achieve a smooth flow over the surface. This is an iterative process in which each iteration involves a number of steps; first modifying the contours of the fuselage cross-sections, then generating the wing-fuselage intersection curve and attaching the wing, creating the grid for this configuration, analyzing the flow and finally visualizing the surface flow pattern. These modifications are also subject to the design constraints and are restricted to the fairing / cowling that fits under the fuselage [22]. The curve editing facilities available in GRIDGEN software has been utilized and the flow analysis were made using the JUEL3D code. Both the original and the modified shapes of some typical cross-sections of the fuselage and a particular section after the wing is added are shown in Fig.13 and Fig.14 respectively. Fig. 15 shows the sections of the original and modified fuselage. After modification the wing-fuselage configuration has been analyzed and the streamlines are shown in Fig.16 along with those obtained for the original one. The streamline pattern shows that the modified configuration has a smoother flow pattern and does not have the clustering of streamlines on the rear fuselage as seen in the original one.

Conclusions

It has been shown here that the CFD is now able to simulate the flow past realistic aerospace configurations. It can thus play a significant role not only in the study of

complex fluid flow structure but also in the design and development of an aircraft. In the near future, with further improvement in computer technology and numerical algorithms, CFD will be able to simulate even more complex flows with less turnaround time and thus become a robust and reliable design tool by making design process faster, more accurate and less expensive.

Acknowledgements

Technical help received from Mrs. K. Dhanalakshmi during the preparation of this manuscript is gratefully acknowledged. Some of the results reported here are from my colleagues at NAL and the author takes this opportunity to thank all of them.

References

- Magnus, R. and Yoshihara, H., "Inviscid Transonic Flow Past Airfoils", *AIAA Journal*, Vol.8, pp.2157-2162, 1970.
- Murman, E. M. and Cole, J. D., "Calculation of Plane Transonic Flows", *AIAA Journal*, Vol.9, pp.114-121, 1971.
- Pearcy, H. H., "The Aerodynamic Design of Section Shapes for Swept Wings", *Advances in Aeronautical Sciences*, Vol.3, pp.277-322, 1962.
- Nieuwland, G. Y. and Spee, B. M., "Transonic Shock-free Flow, Fact or Fiction"? AGARD Conference Proceedings, No. 35, NLR MP 68004U, Netherlands, 1968.
- Spee, B. M. and Uijlenhoet, R., "Experimental Verification of Shock-free Transonic Flow Around Quasi-elliptical Aerofoil Sections", NLR Report MP 68003U, Amsterdam, 1968.
- Bauer, F., Garabedian, P., Korn, D. and Jameson, A., "Supercritical Wing Sections II", *Lecture Notes in Economics and Mathematical Systems*, Vol.108, Springer-Verlag, 1975.
- Chakrabarty, S. K. and Dhanalakshmi, K., "Navier-Stokes Analysis of Korn Aerofoil", *Acta Mechanica*, Vol.118, pp.235-239, 1996.
- Ferrari, C. and Tricomi, F. G., "Transonic Aerodynamics", Academic Press, New York and London, 1968.
- Ramabhadran, S., "Supercritical Aerofoil Design Using Electrical Analogy Technique", M. Sc. (Engg.) Theses, Department of Aerospace Engineering, Indian Institute of Science, January, 1981.
- Srilatha, K.R., Dwarakanath, G.S. and Ramamoorthy, P., "Design of a Natural Laminar Flow Aerofoil for the Light Transport Aircraft", *Acta Mechanica*, Vol.85, pp. 251-258, 1990.
- Srilatha, K.R., Dwarakanath, G.S. and Ramamoorthy, P., "Design of a Natural Laminar Flow Aerofoil for a Light Aircraft", *Journal of Aircraft*, Vol.27, No.11, pp.966-968, 1990.
- Hazra, S. B., "An Efficient Method for Aerodynamic Shape Optimization", *AIAA Paper 2004-4628*, 10th AIAA/ISSMO Multidisciplinary Analysis and Optimization Conference, August 30 - September 01, Albany, New York, 2004.
- Niyogi, P. and Mitra, R., "Approximate Shock-free Transonic Solution for a Symmetric Profile at Zero Incidence", *AIAA Journal*, Vol.11, pp.751-754, 1973.
- Chakrabarty, S. K., "An Analytical and Numerical Study of Plane Transonic Profile Flow at Zero and Non-zero Incidence", Ph.D. Thesis, Jadavpur University, Kolkata, 1974.
- Chakrabarty, S. K., "Approximate Shock-free Transonic Solution for Lifting Aerofoils", *AIAA Journal*, Vol.13, No.8, pp.1094-1097, 1975.
- Niyogi, P., "Integral Equation Method in Transonic Flow", *Lecture Notes in Physics*, Vol.157, Eds. Ehlers, J. et al, Springer-Verlag, Berlin, Heidelberg, New York, 1982.
- Ramaswamy, M. A. and Desai, S. S (eds), *Proceedings of Workshop on "Transonic Aerodynamics"*, National Aerospace Laboratories, Bangalore, December, 1976.
- Desai, S. S., "A Suitable CFD?", *Computational Fluid Dynamics Journal*, Vol.10, No.4, pp.455-465, 2002.
- Desai, S. S., "Relative Roles of Computational Fluid Dynamics and Wind Tunnel Testing in the Develop-

ment of Aircraft", Current Science, Vol.84, No., pp. 49-64, 2003.

- 20. Chakrabarty, S. K., Mathur, J. S. and Dhanalakshmi, K., "Application of Advanced CFD Codes for Aircraft Design and Development at NAL", Journal of Aerospace Sciences and Technologies, Vol.55, No.1, pp.74-88, February, 2003.
- 21. Chakrabarty, S. K., Dhanalakshmi, K. and Ramesh, V., "Navier-Stokes Analysis of GA(W)-2 Aerofoil with Deflected Flap and Redesign of HANSA Flap for Better Performance", Computational Fluid Dynamics Journal, Vol.12, No.1, pp. 89-97, April, 2003.

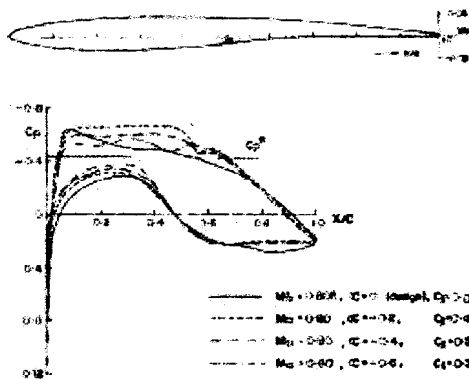


Fig. 1 Shock-free aerofoil designed at NAL using RACM and analysis results for different flow conditions

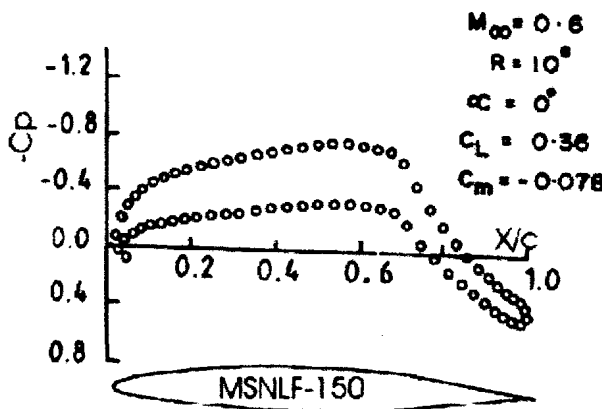


Fig. 2 Design of a natural laminar flow aerofoil at NAL

- 22. Mathur, J.S., Dhanalakshmi, K. and Chakrabarty, S.K., "Application of Advanced CFD Codes for the Design and Development of SARAS Aircraft", Journal of Aerospace Sciences and Technologies, Vol.55, No.3, pp.174-185, August, 2003.
- 23. Chakrabarty, S.K., Dhanalakshmi, K. and Mathur, J.S., "Navier-Stokes Analysis of Vortex Flow Over a Cropped Delta Wing", Acta Mechanica, Vol.131, pp.69-87, 1998.
- 24. Dhanalakshmi, K., Chakrabarty, S. K., Mathur, J. S. and Ramesh, V., "Computation of Inviscid Flow Past SARAS Aircraft with Side-slip Using a Multi-block Grid", Journal of Aerospace Sciences and Technologies, Vol.56, No. 1, pp. 66-76, February, 2004.

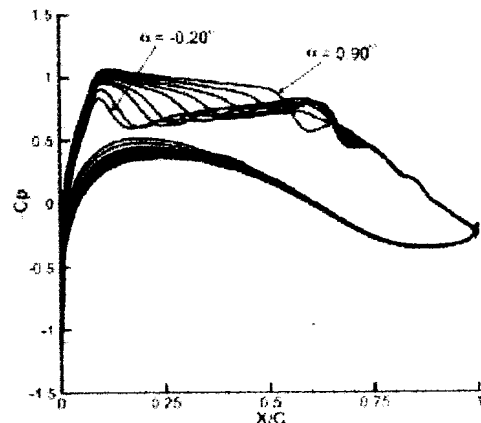


Fig. 3 Effect of angle of attack on surface pressure coefficient on Korn aerofoil at $M_{\infty} = 0.75$, $Re_{\infty} = 5.42 \times 10^6$, $\alpha = 0.20, 0.00, 0.25, 0.35, 0.50, 0.60, 0.70, 0.80, 0.90$ degrees

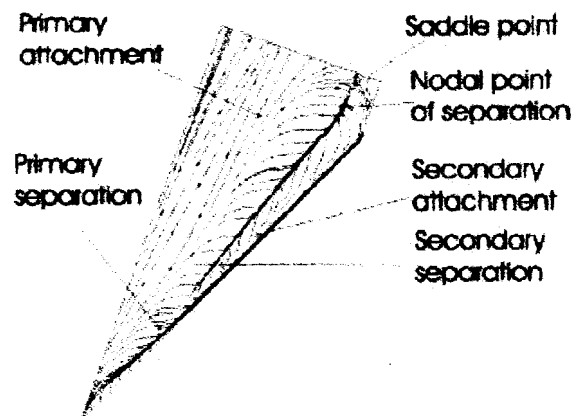


Fig. 4 Skin-friction lines on the upper surface of cropped delta wing at $M_{\infty} = 0.85$, $\alpha = 10^\circ$, $Re_{\infty} = 2.38 \times 10^6$

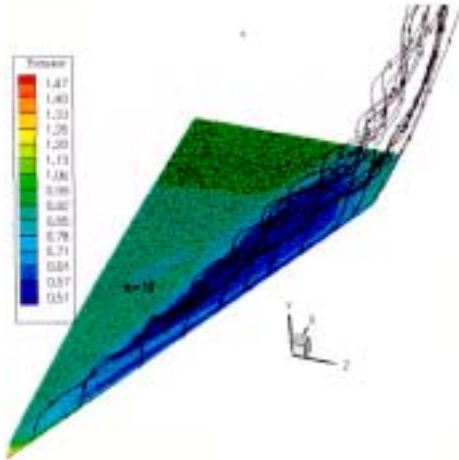


Fig. 5 Surface pressure contour and streamlines showing primary and secondary vortices

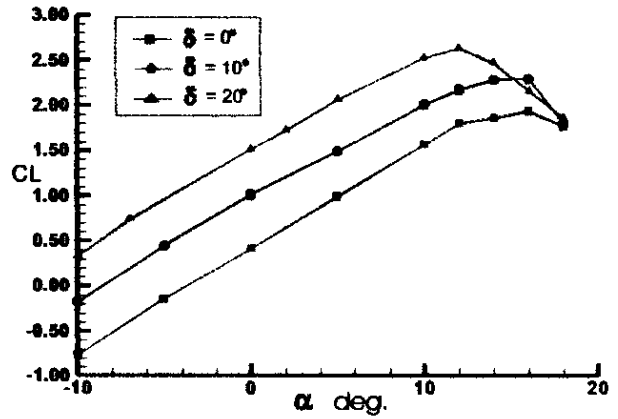


Fig. 9 Lift coefficient for HANSA-3 aerofoil with modified flap at $M_\infty = 0.3$, $Re_\infty = 2.0 \times 10^6$

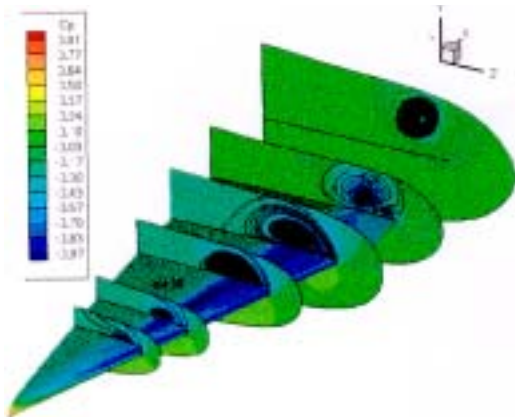


Fig. 6 Cp Contours and particle traces on the cross-flow planes and Cp contours on the wing surface for $M_\infty = 0.85$, $\alpha = 10^\circ$, $Re_\infty = 2.38 \times 10^6$

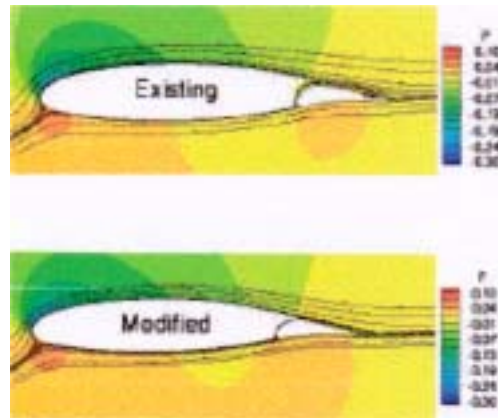


Fig. 10 Streamlines and pressure contours of the existing HANSA-3 and modified flap configurations at $M_\infty = 0.3$, $\delta = 0^\circ$, $\alpha = 10^\circ$, $Re_\infty = 2.0 \times 10^6$

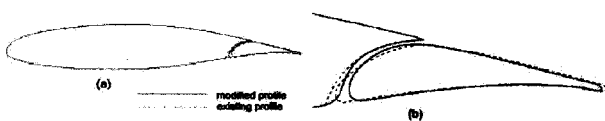
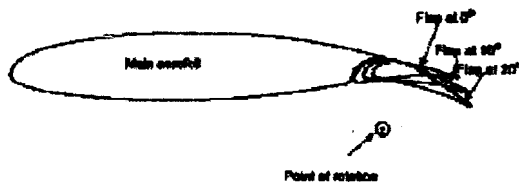


Fig. 7 Comparison of existing and modified profiles of HANSA-3 aerofoil with flap configuration: (a) Full configuration, (b) Enlarged view near the gap and flap



Point of rotation :
 Existing : (0.826,-0.0766) or (1079mm, 100mm)
 Modified: (0.830,-0.1200) or (1084mm,-156mm)

Fig. 8 Redesigned aerofoil and flap configuration with three positions of deflected flap

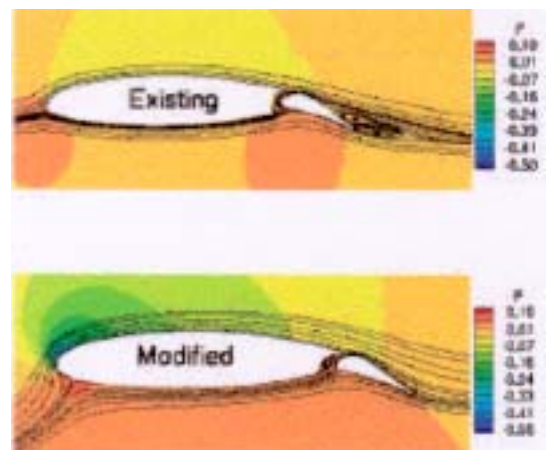


Fig. 11 Streamlines and pressure contours of the existing HANSA-3 and modified flap configurations at $M_\infty = 0.3$, $\delta = 20^\circ$, $\alpha = 10^\circ$, $Re_\infty = 2.0 \times 10^6$

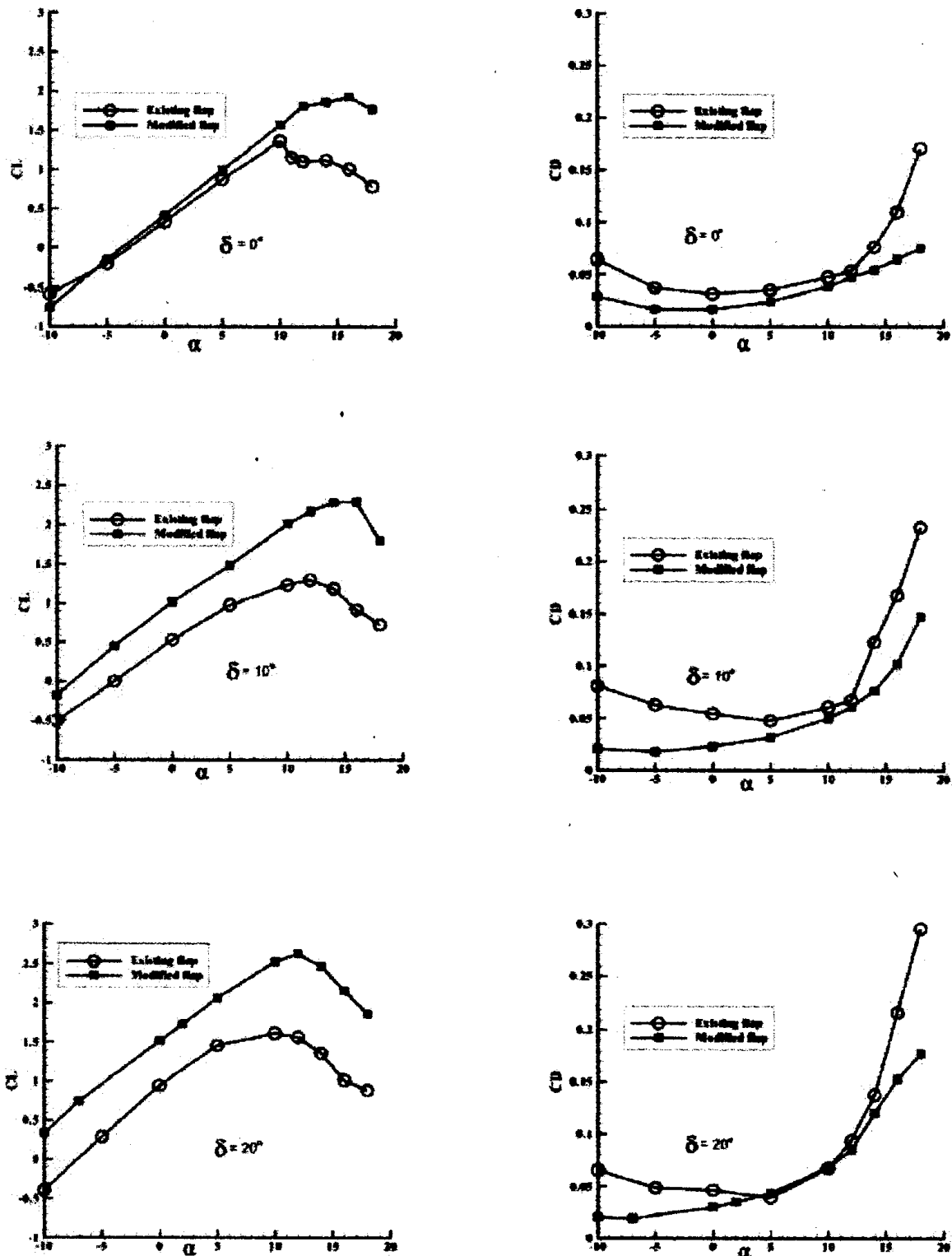


Fig. 12 Comparison of lift and drag coefficients of existing and modified aerofoil-flap configurations of HANSA-3 aircraft for different α at $M_\infty = 0.3$, $Re_\infty = 2.0 \times 10^6$ at three different flap positions

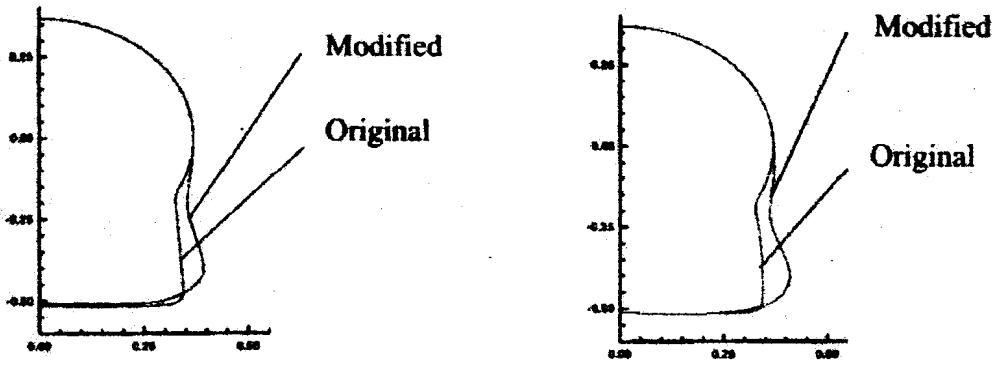


Fig. 13 Typical fuselage sections of SARAS showing original and modified fuselage

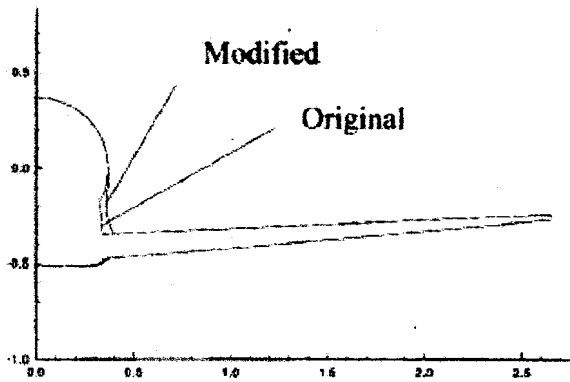


Fig. 14 Typical SARAS fuselage section showing original and modified fuselage with wing also attached

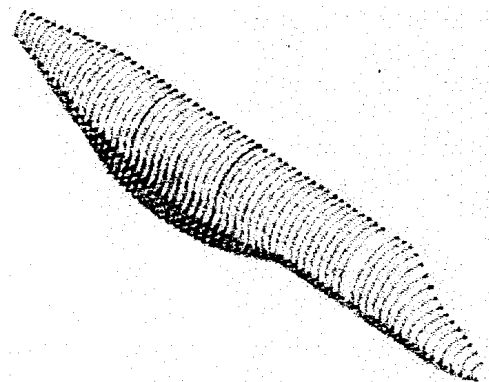


Fig. 15 Fuselage sections showing modifications in the vicinity of the SARAS wing-fuselage junction

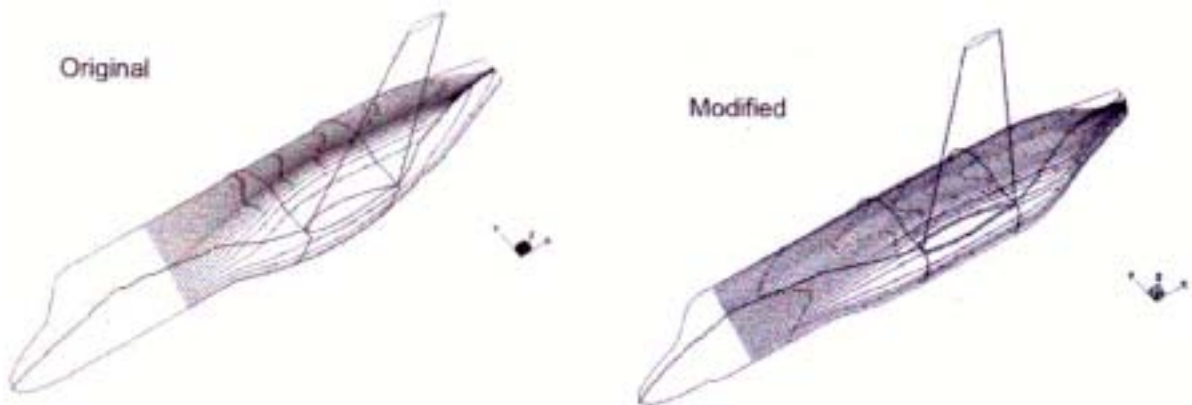


Fig. 16 Surface flow patterns on original and modified SARAS wing fuselage fairings